

# Main Injector RF Requirements for a 1.3 Megawatt 120 GeV Proton Source

Dave McGinnis

May 13, 2006

## INTRODUCTION

Beam loading will dominate the operation of the Main Injector RF system for 120 GeV beam powers greater than 700kW. This note outlines a simple calculation of the RF power requirements in the Main Injector for a 1.3 MW 120 GeV proton source.<sup>1</sup>

## MAIN INJECTOR RF RAMPS

To deliver 1.3MW at 120 GeV, eighteen Booster batches are combined by momentum stacking in the Accumulator and box-car stacking in the Recycler. To load eighteen batches into the Accumulator and Recycler at 15 Hz requires 1.2 seconds. A beam power of 1.3MW would require  $8.2 \times 10^{13}$  protons every 1.2 seconds.<sup>2</sup> A beam power of 650kW would require  $4.5 \times 10^{13}$  protons every 1.33 seconds. The energy ramp used in this note is show in Figure 1. This ramp has a more complicated injection parabola to minimize the RF voltage at injection to avoid possible accidental damage to the bias tuner. The ramp acceleration time is 0.6 seconds with a maximum acceleration rate of 240 GeV per second.

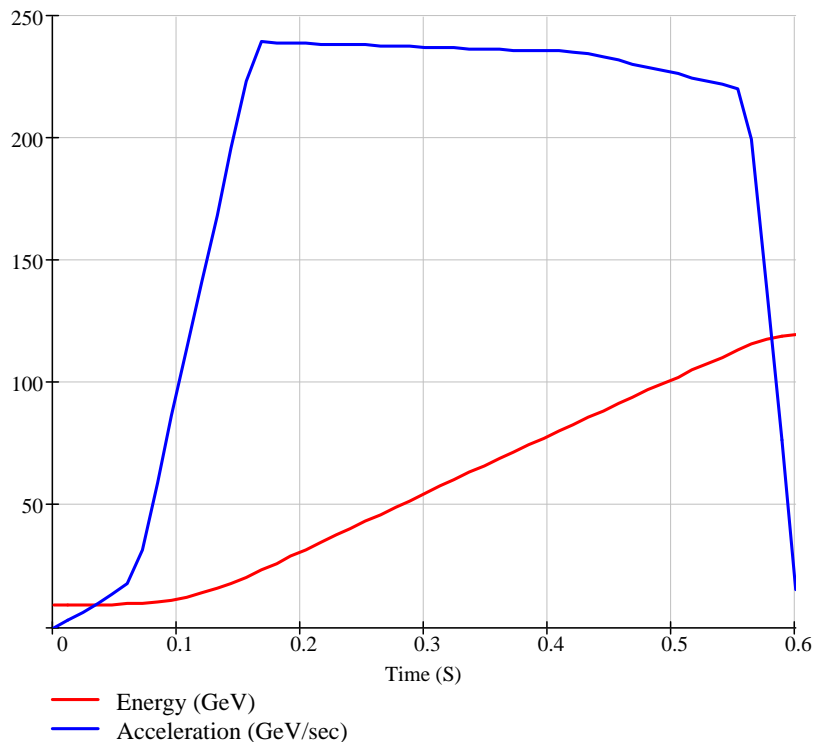


*Figure 1. Main Injector Energy Ramp*

<sup>1</sup> "A 2MW Multi-Stage Proton Accumulator", Dave McGinnis, Fermilab Beams Document 1782, September, 2005

<sup>2</sup> "Proton Source Scaling Laws", Dave McGinnis, Fermilab Beams Document 1783, May 2006

The RF voltage curve is determined by the acceleration rate and the bucket area. The intensity of each Booster batch is  $4.6 \times 10^{12}$  protons resulting in a total intensity of  $8.2 \times 10^{13}$  protons injected into the Main Injector. The longitudinal emittance of the beam is set by the momentum stacking process in the Accumulator. The momentum stacking process dilutes the longitudinal emittance by about twenty percent. For a total of eighteen Booster batches loaded into the Main Injector, it would be necessary to stack three Booster batches into the Accumulator and six Accumulator batches into the Recycler. The longitudinal emittance of a 53MHz bunch in the Booster is 0.08eV-s. A twenty percent emittance dilution for stacking three Booster batches results in an equivalent emittance of 0.38eV-s for a 53 MHz RF bucket. It will be assumed that momentum dilution in the Recycler will not increase the longitudinal emittance above 0.5eV-s per 53MHz bucket. An RF bucket area of 0.75eV-s in the Main Injector should be sufficient to contain the bunches at injection. After transition, the bucket area should be raised to 1.8 eV-s to contain the tails created during transition crossing. The RF voltage is shown in Figure 2. The bucket area shown is held constant at 1.8 eV-s for most of the ramp except before transition and near extraction. To hold a 1.8eV-sec bucket area during these times would require the total RF voltage to drop unrealistically low. A bucket area of 1.55eV-s at 0.216 sec would keep the total RF voltage below 4 MV.

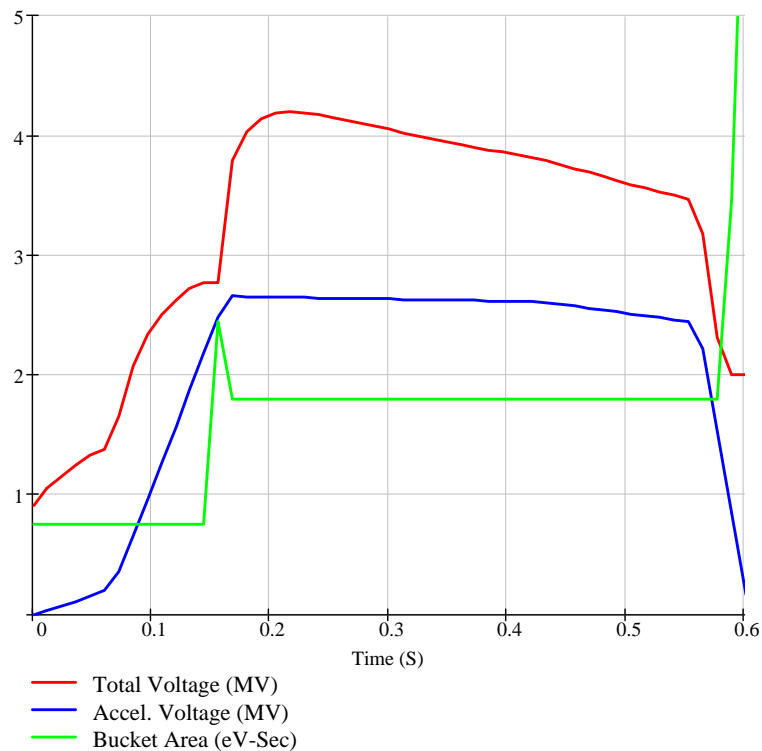


Figure 2. RF voltage curves.

#### RF BEAM CURRENT.

The RF beam current is a function of the bunch length. If the bunches are long then the amount of beam current that the RF cavities see will be reduced. However because of the large synchronous phase angle in the Main Injector during acceleration, the bunch length is very short even for full RF buckets. Particles execute trajectories in phase space according to:

$$H = \frac{A}{2} y^2 + B(\phi \sin \phi_s \mp (\cos(\phi) - 1)) \quad (1)$$

where H is a constant for a given trajectory and the top sign is used above transition. The normalized particle energy deviation  $y$  is:

$$y = \frac{\Delta E}{\omega_{rf}} \quad (2)$$

which has units of eV-s. The coefficients A and B are given as:

$$A = \left( \frac{\omega_{rf}}{\beta} \right)^2 \frac{\eta}{E_s} \quad (3)$$

$$B = \frac{qV_{rf}}{2\pi h} \quad (4)$$

The bucket edge is given by the value of H that satisfies:

$$\begin{aligned} \phi &= \pm(\phi_s - \pi) \\ y &= 0 \end{aligned} \quad (5)$$

The voltage for a given bucket area reaches its largest value at 0.216s as shown in Figure 2. The bucket shape at 0.216s for a 1.8 eV-s bucket is shown as the blue trace in Figure 3.

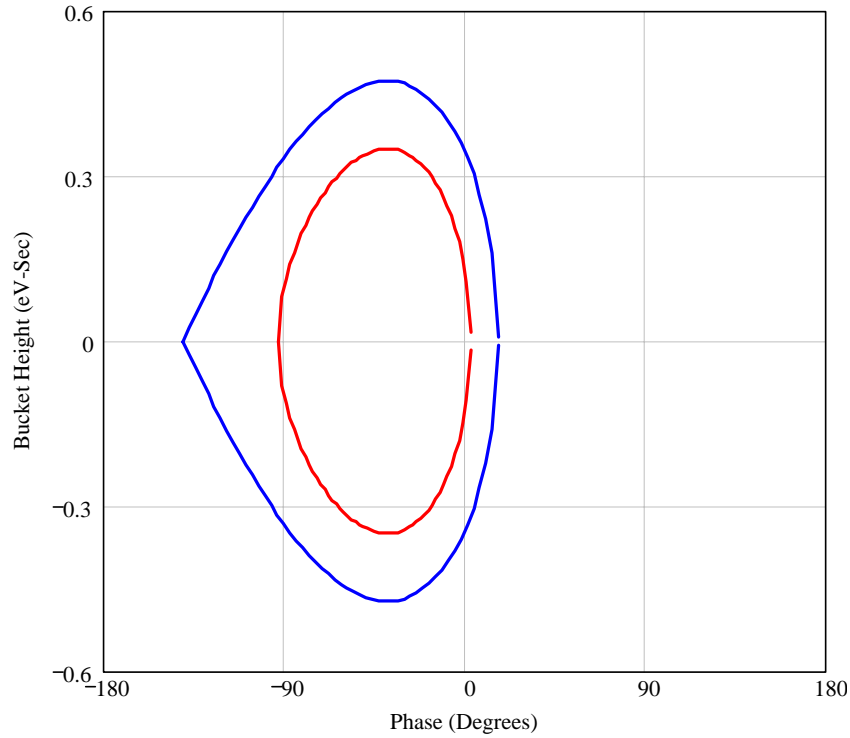


Figure 3. Phase space of a 1.8eV-s bucket at 0.216s is shown in blue. The beam edge for a longitudinal emittance of 0.5eV-s is shown in red.

The beam edge for 0.5eV-s longitudinal emittance is shown as the red trace of Figure 3. Even though the bucket is rather full, the bunch only extends along 90 degrees of phase. If the phase space density is uniform, then the RF beam current is given as:

$$i_b = \frac{4I_{dc}}{f_R \epsilon_L} \left| \int_{-\pi}^{\pi} y_e(\phi) e^{j\phi} d\phi \right| \quad (6)$$

where  $y_e$  is the edge of the beam phase space,  $I_{dc}$  is the DC beam current,  $\epsilon_L$  is the longitudinal emittance, and  $f_R$  is the ring fill factor which is 6/7 for the Main Injector. Figure 4 shows the ratio of RF beam current to DC beam current for the voltage profile shown in Figure 3.

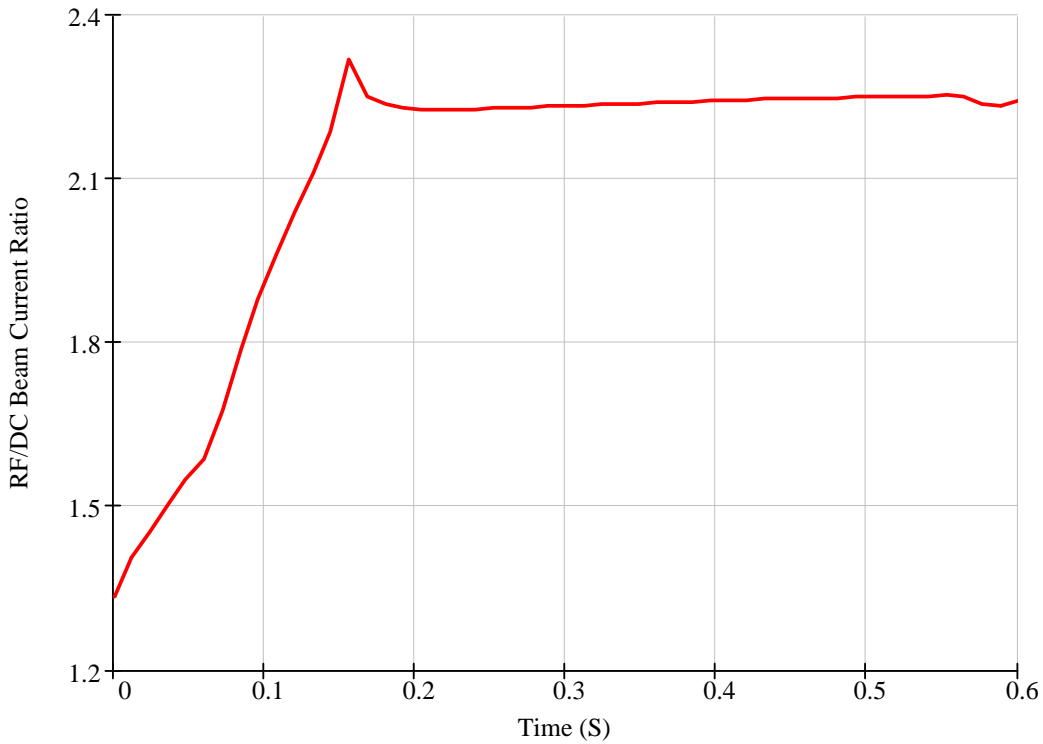


Figure 4. Ratio of RF beam current to DC beam current for a uniform density of 0.5eV-s. The ring fill factor is 6/7.

### BEAM LOADING

The equivalent circuit model for the cavity is shown in Figure 5. The impedance of the cavity is given as:

$$Z_c = R_c \cos(\phi_z) e^{\pm j\phi_z} \quad (7)$$

where  $R_c$  is the real part of the cavity impedance and  $\phi_z$  is the cavity detuning angle. The power amplifier is modeled as a current source  $nI_g$  with internal impedance  $R_g/n^2$ . The coupling of the power amplifier to the cavity is modeled as a step-up transformer with  $n$  turns. For the Main Injector cavities, this step-up ratio is approximately 12~13. The ratio

of the cavity resistance to the generator resistance (as seen by the cavity) is defined as the cavity coupling  $r$ .

$$R_c = rR_g \quad (8)$$

The ratio of the total resistance to the cavity resistance is given as:

$$R = \frac{1}{r+1} R_c \quad (9)$$

For a tetrode power amplifier,  $r \ll 1$ .

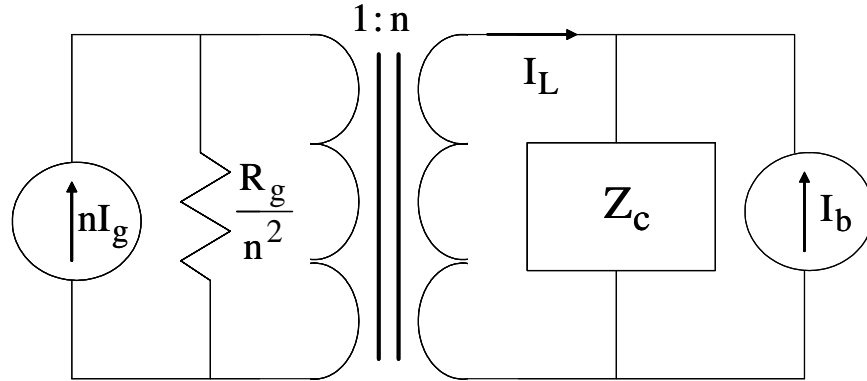


Figure 5. Circuit model for a cavity

The phasor diagram of the cavity circuit above transition is shown in Figure 6. The beam current is given as:

$$I_b = \mp j i_b e^{\mp j \phi_s} \quad (10)$$

The generator current is broken into a component that cancels the beam current ( $-xI_b$ ) and a component in phase with the cavity voltage ( $\Delta i_{gr}$ ).

$$I_g = \Delta i_{gr} \pm j x i_b e^{\mp j \phi_s} \quad (11)$$

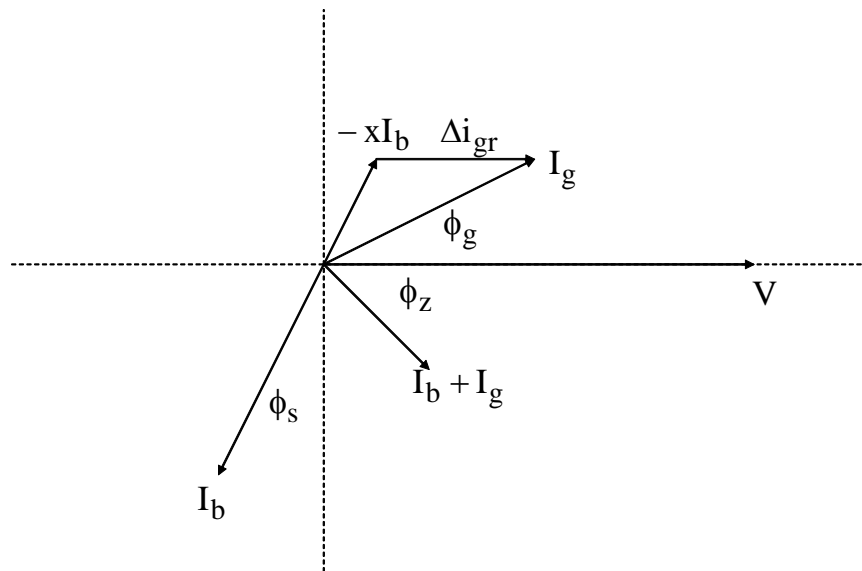


Figure 6. Cavity phasor diagram. The phasor rotates counter-clockwise with time.

The cavity voltage is:

$$V_c = i_b(1-x)R \frac{\cos(\phi_s)}{\tan(\phi_z)} \quad (12)$$

The generator current becomes:

$$I_g = \frac{V_c}{R} + i_b \sin(\phi_s) \pm jx i_b \cos(\phi_s) \quad (13)$$

The current provided by the power amplifier as seen by cavity becomes:

$$I_L = \frac{V_c}{R(r+1)} + i_b \sin(\phi_s) \pm jx i_b \cos(\phi_s) \frac{r+x}{r+1} \quad (14)$$

The power supplied by the power amplifier is:

$$P_L = \frac{1}{r+1} \frac{V_c^2}{2R} + \frac{V_c i_b}{2} \sin(\phi_s) \quad (15)$$

The power dissipated in the cavity is:

$$P_c = \frac{1}{r+1} \frac{V_c^2}{2R} \quad (16)$$

#### ROBINSON STABILITY

The high intensity Robinson threshold requires:

$$\frac{R i_b}{V_c} (1-x) \frac{\sin(2\phi_z)}{\cos(\phi_s)} = \frac{2}{\sigma^2} \quad (17)$$

$$\sigma^2 > 1$$

Using the equations for the cavity voltage and Robinson threshold, the constraint on cavity de-tuning becomes:

$$\sin^2(\phi_z) = \frac{1}{\sigma^2} \cos^2(\phi_s) \quad (18)$$

The stability factor as a function of cavity voltage and beam current becomes:

$$\sigma^2 = \left( \frac{V_c}{i_b R (1-x)} \right)^2 + \cos^2(\phi_s) \quad (19)$$

There are two approaches to keep the beam stable for large beam currents. The simplest approach is to reduce the cavity resistance or the cavity Q with an external load. This approach permits the generator current to be in phase with the cavity voltage so that the power amplifier sees a real load which minimizes plate dissipation. However, the benefits of this approach are offset by the increased power requirements of having to generate more power just to develop the desired cavity voltage.

The other approach is to cancel some of the beam current with a generator current. This cancellation can be done with either a feed-forward system or RF feedback. The advantage to this approach is that there is no extra power wasted in an external load. The disadvantages of the approach are the complexity of the feed-forward or feedback systems and the generator current is out of phase with the cavity voltage so that the power amplifier does not see a real load.

#### REQUIRED POWER AMPLIFIER POWER

The power required from the power amplifier will be calculated in this section. The parameters used in this calculation are shown in Table 1. The stability factor ( $\sigma^2$ ) for 700kW and 1.3 MW of beam power is shown in Figure 7. The active beam loading curves, shown in red, use 90% beam loading compensation. Ninety percent compensation is equivalent to 19dB of loop gain of RF feedback. The stability factor resulting from resistively loading the cavities to a Q of 570 (14% of nominal) is shown in the blue traces.

The delivered RF current from the power amplifier as seen by the cavity is shown in Figure 8. The delivered RF power from the power amplifier is shown in Figure 9. The load, de-tuning, and synchronous phase angles for 90% beam-loading compensation are shown in Figure 10. Even though resistive loading has less than a factor of two less stability as compared to active beam loading compensation, resistive loading requires almost double the RF current and power from the power amplifier.

The current and power calculated in Figure 8 and Figure 9 were calculated for constant beam-loading compensation (and resistive loading) throughout the acceleration cycle. It would be possible to vary the amount of beam-loading compensation through the acceleration cycle to keep a constant Robinson stability factor. Figure 11 shows the reduction in beam-loading compensation and resulting tube current reduction if the RF system is run at a constant Robinson stability factor of two. Figure 11 shows that there is probably not enough reduction to justify varying the beam-loading compensation throughout the acceleration cycle.

Parameter	Value	Units
RF Frequency	53	MHz
Harmonic	588	
$\gamma_t$	21.8	
Ramp time	0.6	S
Cycle Time	1.33	S
Number of Cavities	20	
R/Q	100	$\Omega$
Q	4000	
Coupling	0.1	
Coupler Step-up Ratio	12.5	
Longitudinal Emittance	0.5	eV-S
Ring Filling Factor	0.86	
Beam Loading Compensation	90%	
Resistive Loading	14%	

*Table 1. Main Injector RF Parameters*

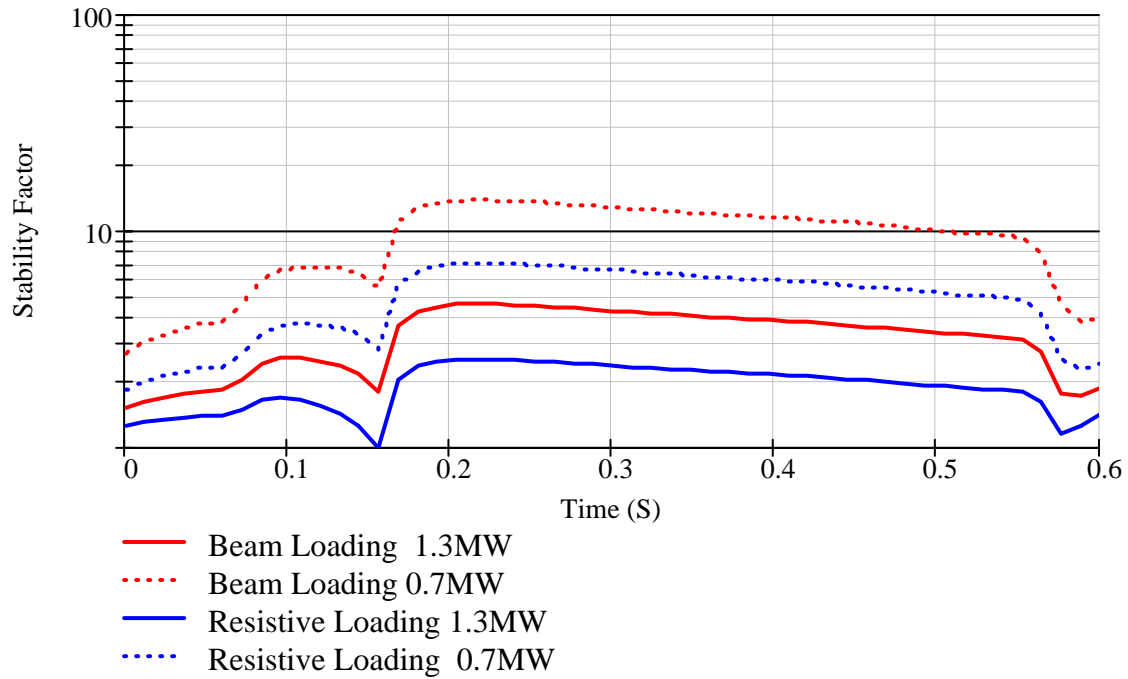


Figure 7. Stability factor ( $\sigma^2$ ) for 90% active beam loading compensation (red traces) compared to 14% resistive cavity loading (effective  $Q=570$ ) (blue traces).

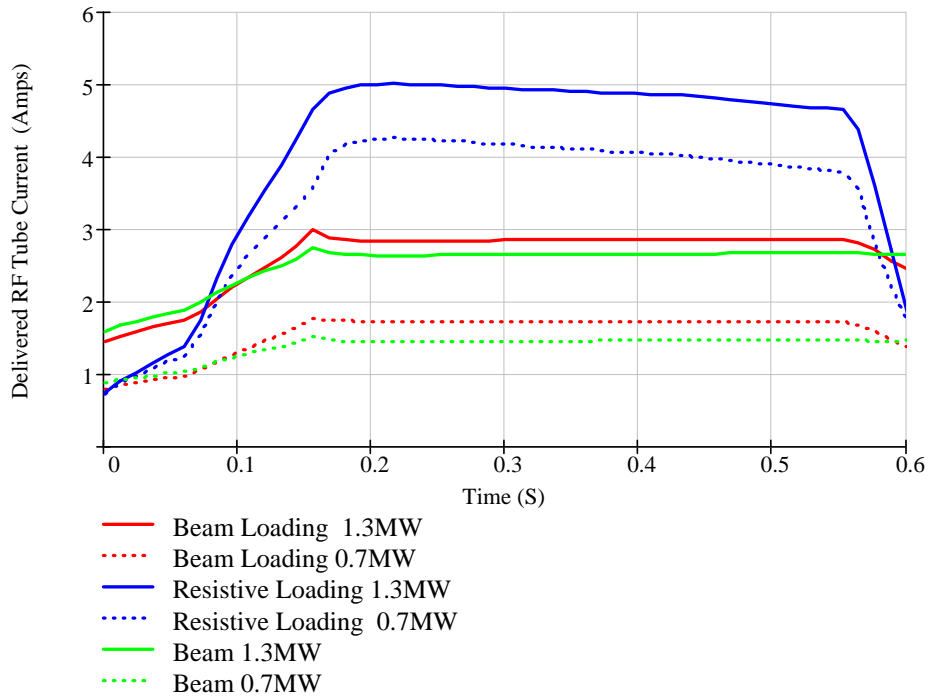


Figure 8. Delivered RF current from the power amplifier as seen by the cavity for 90% beam loading compensation (red traces) and 14% resistive cavity loading (effective  $Q=570$ ) (blue traces). The green traces are the beam current as seen by the cavity.

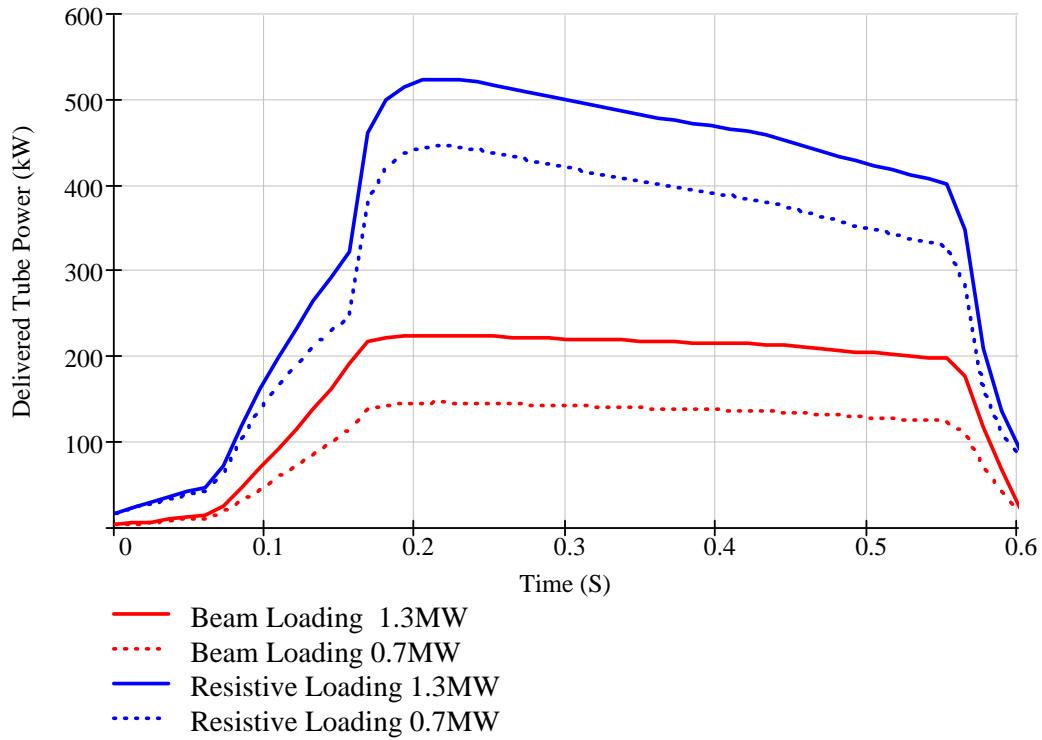


Figure 9. Delivered RF power by the power amplifier for 90% beam loading compensation (red traces) and 14% resistive cavity loading (effective  $Q=570$ ) (blue traces).

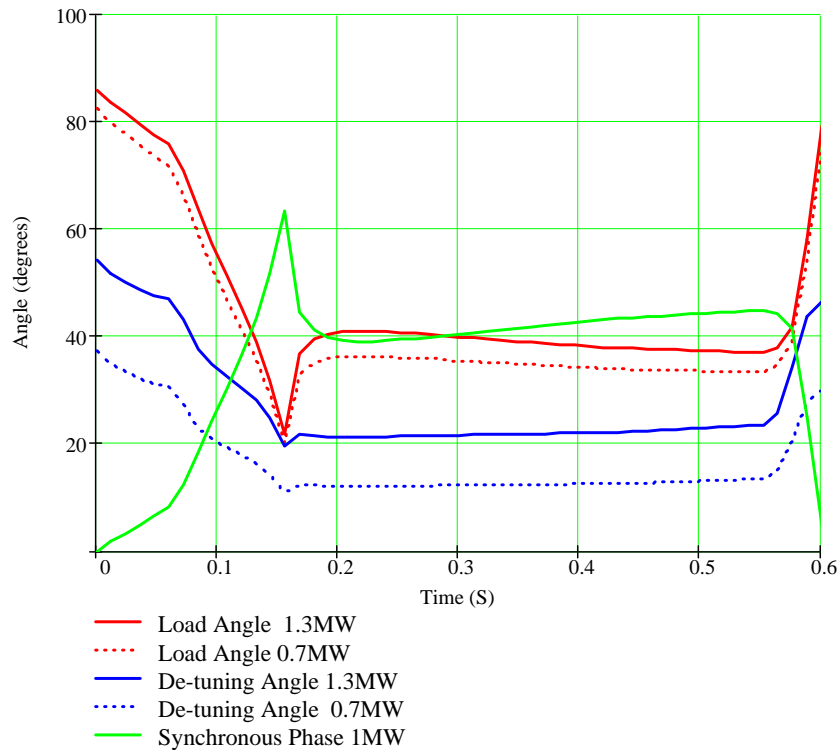


Figure 10. Load, de-tuning, and synchronous phase angles through the acceleration cycle for 90% beam-loading compensation.

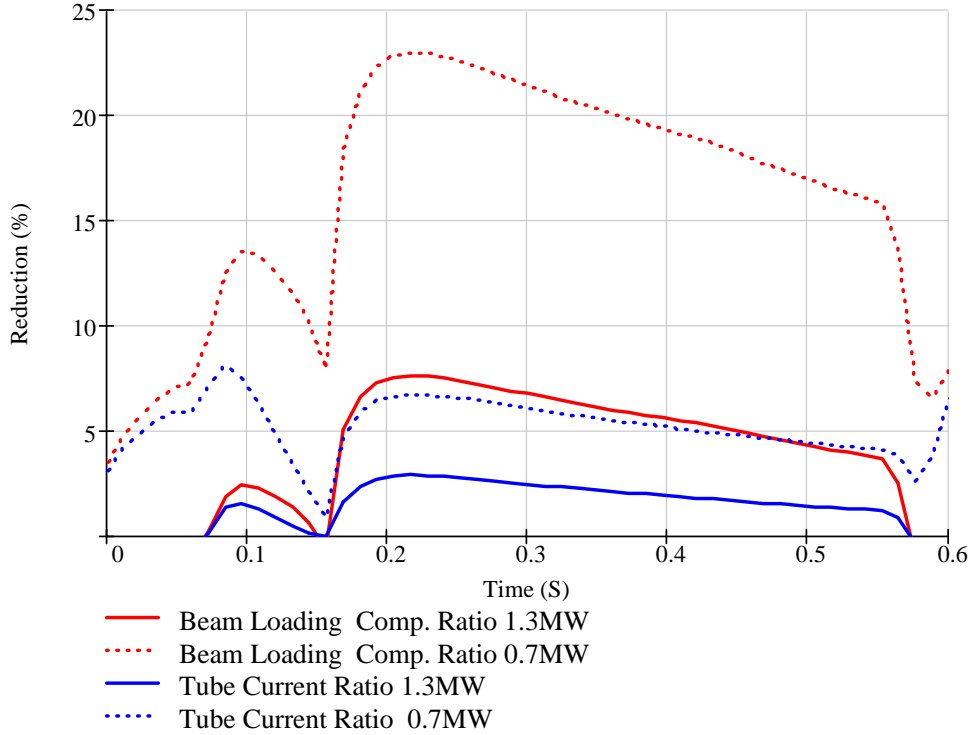


Figure 11. Beam loading compensation (red traces) and tube current (blue traces) reduction for variable beam-loading compensation for a Robinson stability factor of two compared to a constant 90% beam loading compensation.

#### POWER AMPLIFIER CHARACTERISTICS

A Main Injector Cavity is powered single ended by a single Eimac Y-567B tetrode mounted directly on the cavity. The cavity has an additional port to mount another tube so that cavity can be driven in the push-pull mode. The ratings of the tetrode in Class C operation are shown in Table 2. The constant anode current curves for the tube are shown in Figure 12.

Because the RF anode current as a function of RF anode voltage has been calculated above, it is easier to compute the tube operating points if the tube curves are given in the constant grid voltage form. To perform this transformation, the anode current, for anode voltages above 4kV, is fitted to the following function:

$$I_a = \left[ K_a \left( V_g + \frac{V_a}{\mu_a} + \frac{V_s}{\mu_s} \right) \right]^m \quad (20)$$

Figure 13 shows the fit compared to the data at two separate anode voltages for the following parameters:

$$I_a = \left[ 0.012 \left( V_g + \frac{V_a}{700} + \frac{1250V}{3.8} \right) \right]^{2.732} \quad (21)$$

For a constant screen current, the relationship between grid voltage and anode voltage was fit to the following form:

$$V_g = -v_0(I_s) e^{-\frac{V_a}{v_1(I_s)}} + v_2(I_s) \quad (22)$$

Where  $v_0, v_1, v_2$  were empirically determined from the curves in Figure 12 and are listed in Table 3. The constant current curves developed from the models in Eqn. 21-22 are shown in Figure 14

	Maximum	Typical	
Plate Voltage	22	20	kV
Screen voltage	2500	1500	V
Grid voltage	-1500	-800	V
Plate current	20	15.2	A <sub>dc</sub>
Plate Dissipation	150	84	kW
Screen Dissipation	1750	850	W
Grid Dissipation	500	100	W
Output Power		220	kW

Table 2. Ratings for the Eimac Y-567B Tetrode operating as a Class C radio frequency power amplifier

Screen Current	0.2	0.5	1	2	4.1	6	10	14	A
$v_0$	495	739	725	711	726	1749	1196	848	V
$v_1$	1959	9007	3845	2842	3058	10537	7010	6694	V
$v_2$	29	474	354	341	457	1590	1145	919	V

Table 3. Coefficients for screen current fit.

GROUND-CU GRID  
CONSTANT CURRENT CHARACTERISTICS

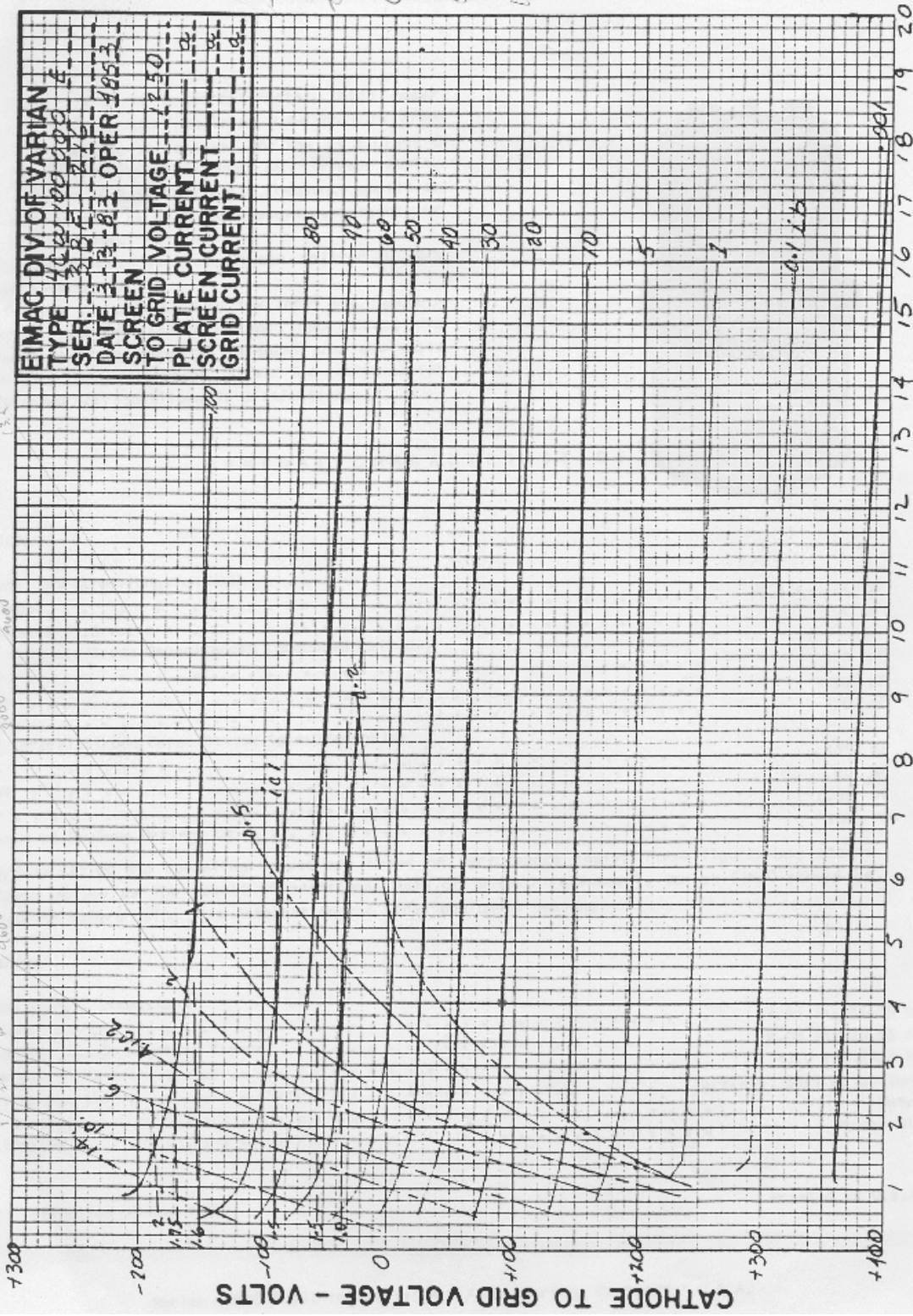


PLATE TO GRID VOLTAGE - KILOVOLTS

Figure 12. Constant anode current curves for the Y-567B tetrode.

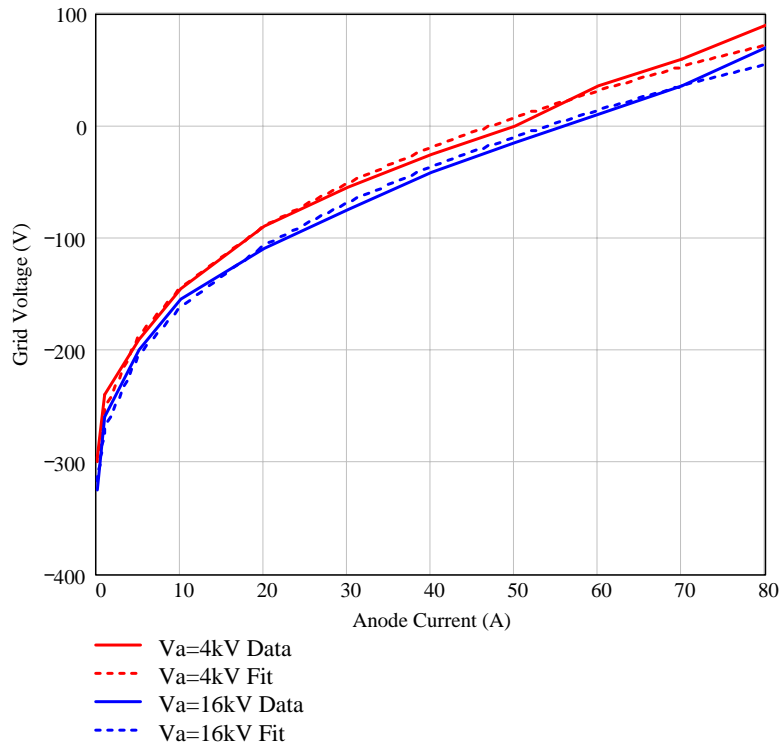


Figure 13. Anode current fit vs. grid voltage for an anode voltage of 4kV (red curves) and 16kV (blue curves)

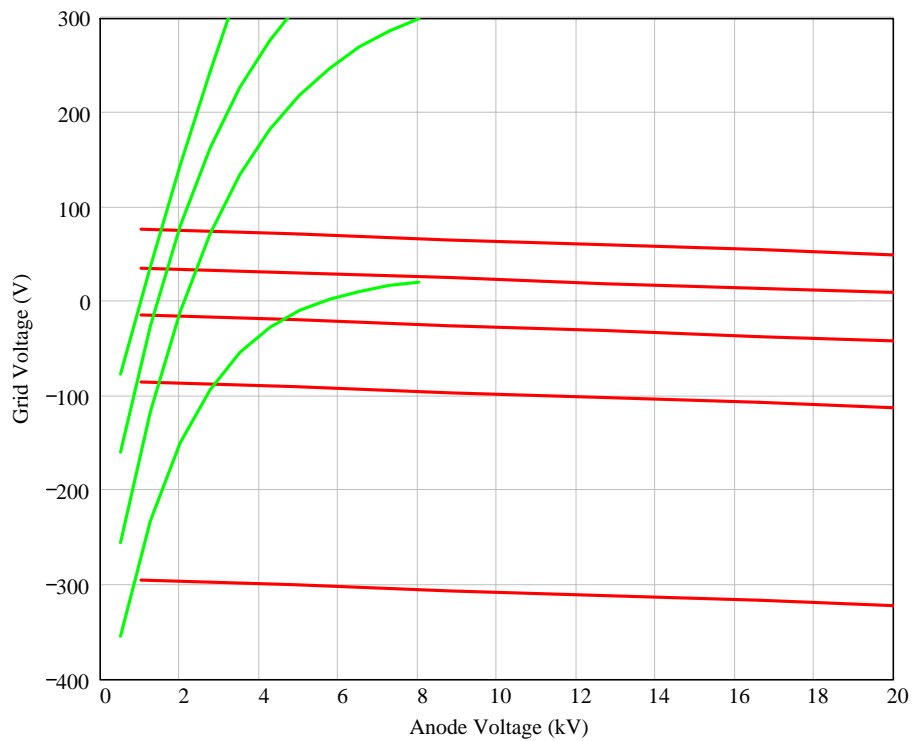


Figure 14. Constant current curves fits for the Y-567B tetrode. The red traces are for constant anode current of 0.1A, 20A, 40A, 60A, and 80A. The green traces are constant screen current of 0.2A, 2A, 4A, and 6A.

### POWER AMPLIFIER OPERATING POINT

. The rest of the note will assume that the RF system is using 90% of active beam loading compensation. The anode voltage is given as:

$$V_a(t) = \frac{V_{tot}}{nN_{cav}} (\cos(\omega_{rf} t) + 1) + V_{a \min} \quad (23)$$

where  $n$  is the coupler step-up ratio,  $V_{tot}$  is the total RF voltage applied to the beam, and  $N_{cav}$  is the number of cavities, The minimum anode voltage  $V_{a \min}$  will be chosen to be 3kV in this note so that the tube does not draw excessive screen current. The modulator will have to provide a DC anode bias:

$$V_{aDC} = \frac{V_{tot}}{nN_{cav}} + V_{a \min} \quad (24)$$

The anode bias voltage per cavity is shown in Figure 16. The grid voltage has the form

$$V_g(t) = V_{gAC} \cos(\omega_{rf} t + \phi_g) + V_{gDC} \quad (25)$$

The grid voltage phase and amplitude must be adjusted to provide the desired anode current for a given anode voltage so that

$$\frac{V_{tot}}{N_{cav} R_c} + i_b \sin(\phi_s) = \frac{n_{tube}}{n} 2f_{rf} \int_{-\frac{1}{2f_{rf}}}^{\frac{1}{2f_{rf}}} I_a(V_g(t), V_a(t)) \cos(\omega_{rf} t) dt \quad (26)$$

$$\frac{r+x}{r+1} i_b \cos(\phi_s) = -\frac{n_{tube}}{n} 2f_{rf} \int_{-\frac{1}{2f_{rf}}}^{\frac{1}{2f_{rf}}} I_a(V_g(t), V_a(t)) \sin(\omega_{rf} t) dt \quad (27)$$

where  $n_{tube}$  is the number of tetrodes mounted to each cavity.

The DC grid bias determines how efficient the amplifier will operate. A large negative grid bias pushes the amplifier into a more efficient Class C operation. However, the smaller conduction angle requires a larger peak anode current to provide the desired RF anode current. Figure 15 shows the anode dissipation (red trace) and the peak anode current (green trace) as a function of the grid bias at 0.216s for a two tubes mounted to each cavity at a beam power of 1.3MW. The anode dissipation quickly increases for grid biases above -250V. In this note a grid bias of -250V will be chosen.

Figure 17 shows tube waveforms at 0.216s for a single tube mounted to each cavity at a beam power of 1.3MW. The grid voltage and anode current as a function of anode voltage for various beam powers and number of tubes mounted to the cavity is shown in Figure 18 and Figure 19. The DC anode current is calculated as:

$$I_{aDC} = f_{rf} \int_{-\frac{1}{2f_{rf}}}^{\frac{1}{2f_{rf}}} I_a(V_g(t), V_a(t)) dt \quad (28)$$

The DC anode current per tube throughout the acceleration cycle is shown in Figure 20. It should be noted that the DC current for single tube at 1.3 MW of beam power is slightly above the maximum rated value as listed in Table 2.

The anode dissipation per tube is the DC tube power minus the AC power delivered to the load:

$$P_{dis} = V_{aDC} I_{aDC} - \frac{1}{2n_{tube}} \left( \frac{1}{R_c} \left( \frac{V_{tot}}{N_{cav}} \right)^2 + \frac{V_{tot}}{N_{cav}} i_b \sin(\phi_s) \right) \quad (29)$$

The anode dissipation though the cycle is shown in Figure 21. For a single tube at 1.3MW of beam power, the peak anode dissipation is above the maximum rated value for the Y567B tetrodes as given in Table 2. Since the RF is on for 0.6 seconds out of 1.2 seconds (50%), the average anode dissipation for a single tube operating at 1.3MW of beam power is below the maximum rated value for the tube. It should also be noted that at 700kW of beam power, a cavity driven by a single tube has ~50% of the RF power and the anode dissipation as that of a single tube at 1 MW of beam power. The two tubes per cavity configuration is well within the maximum tube specification at 1.3MW of beam power.

The anode dissipation shown in Figure 21 was calculated for an anode voltage bias the changed throughout the acceleration cycle as given by Equation 24. Figure 22 shows the anode dissipation for the case of a constant anode voltage bias. The average anode dissipation for a constant anode voltage bias is still well below the maximum rated specifications so that it is possible to eliminate the anode modulator.

The peak anode current is shown in Figure 23. A single tube configuration at 1.3MW of beam power pushes the peak anode current to ~85A in which the tube can provide as shown in Figure 12. However, as the tube ages, increased drive is needed to maintain the large anode current. Typical experience requires limiting the tube to below 55A of peak anode current to maintain reliable operations. With two tubes attached to a single cavity, the required peak anode current is only 40A. The two tube configuration has sufficient margin to handle beam powers up to 1.5 MW. The peak grid and screen currents though the acceleration cycle are shown in Figure 24 and Figure 25. The DC values of the grid and screen current are well within the tube specifications for all configurations.

## SUMMARY

Active beam loading compensation can achieve larger Robinson stability margins for less RF power than externally loading the RF cavities. It is possible to accelerate 1.3MW of beam power with the current Main Injector RF system driven by a single tube and stay near maximum rated specifications of the current power tetrode if active beam loading compensation is implemented and the power tetrodes are operated in Class C.

However, the peak anode current required by a single tube at 1.3MW of beam power is substantially above normal operating experience for reliable operations. The two tubes per cavity configuration provides substantial operating margin up to a beam power of 1.5 MW. It should be noted that the requirements for 700kW of beam power for a single tube mounted on each cavity does not exceed normal operating parameters.

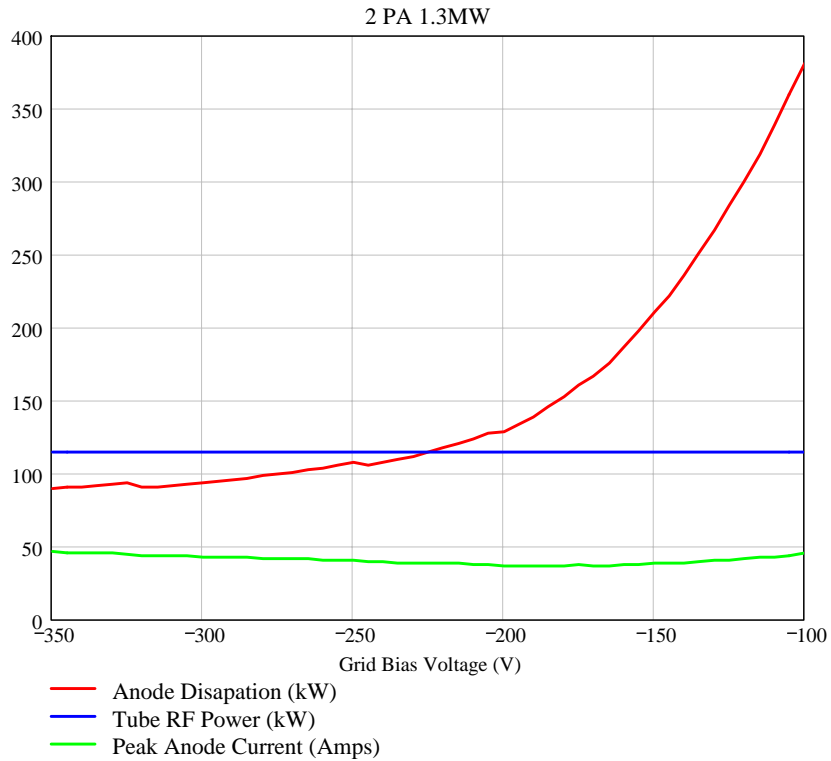


Figure 15. Anode dissipation and peak anode current at 0.216s as a function of the grid bias for a two tubes mounted to each cavity using 90% of active beam loading compensation at a beam power of 1.3MW.

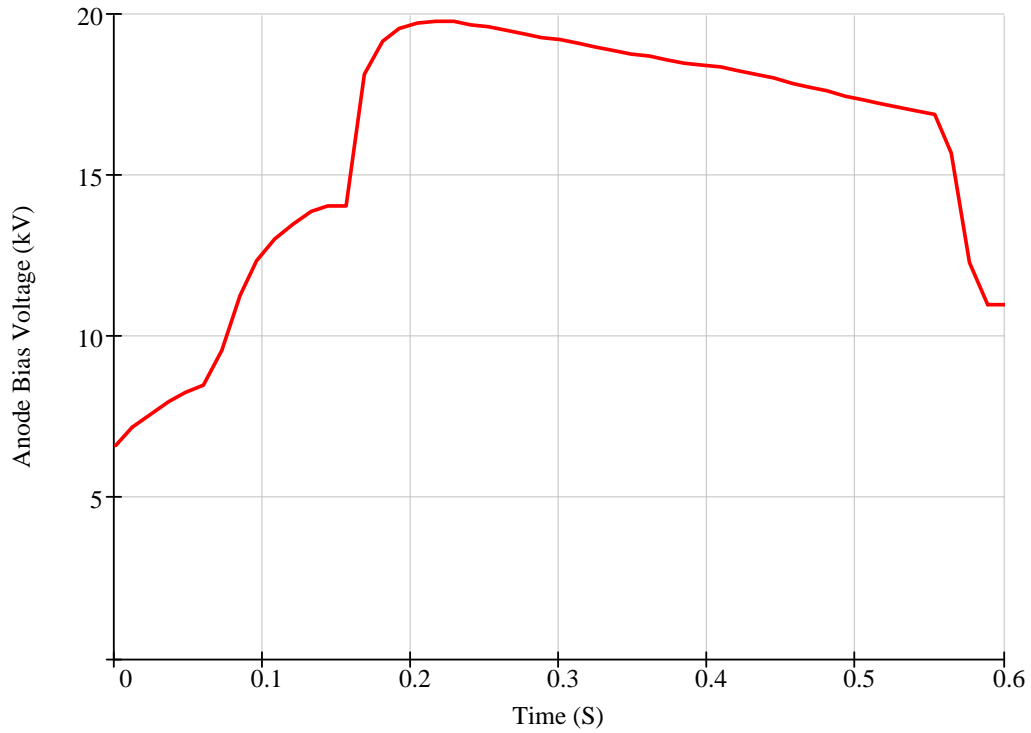


Figure 16. Anode bias voltage

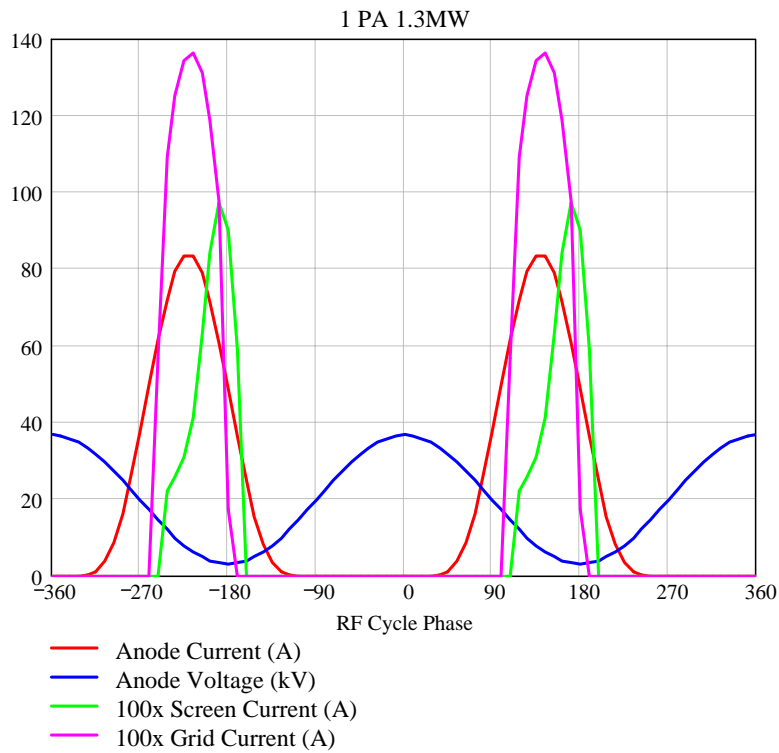


Figure 17. Tube waveforms at 0.216s for a single tube mounted to each cavity at 1.3MW of beam power. The screen (green trace) and grid (magenta trace) currents are multiplied by 100 to fit on the vertical scale.

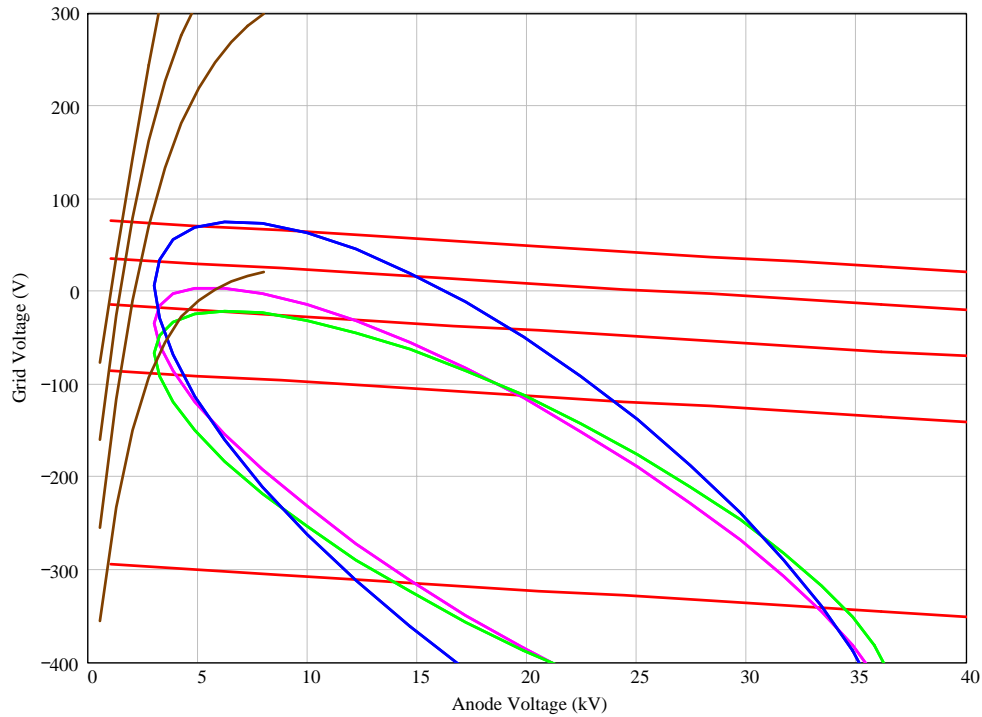


Figure 18. Grid voltage vs. anode voltage at 0.216s. The red and brown traces are constant anode and screen current curves as shown earlier in Figure 14. The trajectory for 1.3MW of beam power and a single tube mounted to each cavity is shown in blue, for two tubes mounted to each cavity is shown in green, and for a single tube with 700kW of beam power is shown in magenta.

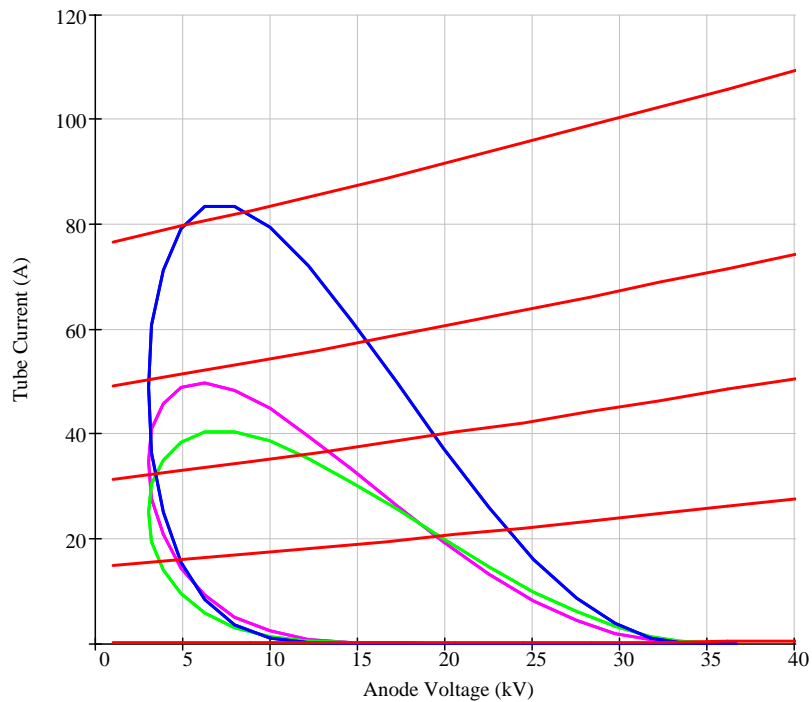


Figure 19. Anode current vs. anode voltage at 0.216s. The red traces are constant grid voltages -325V, -110V, -42V, 10V, 70V.

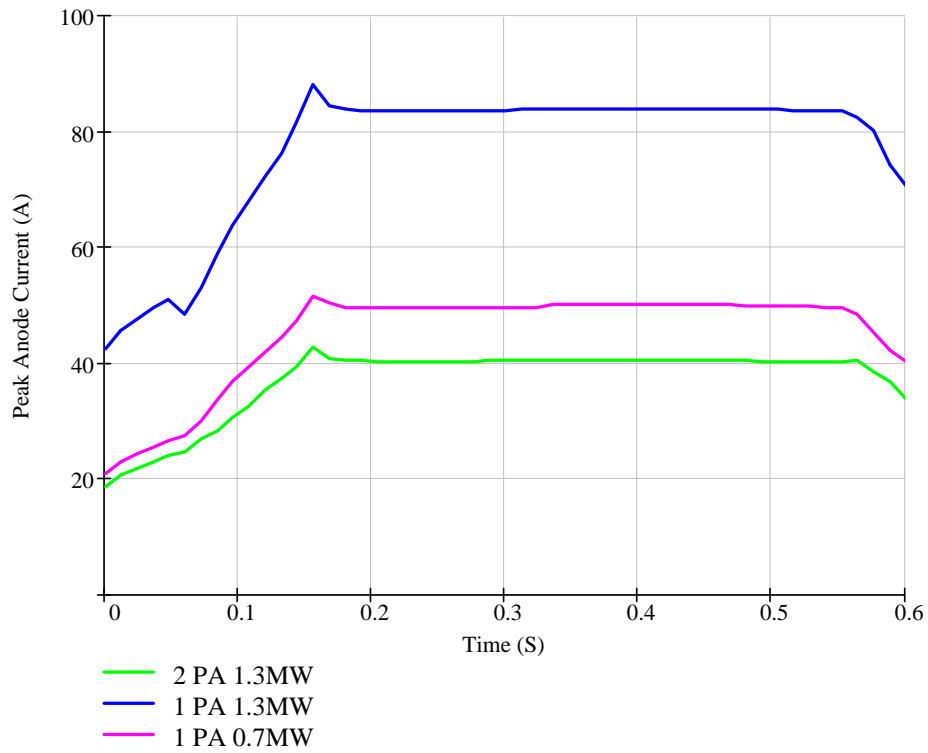


Figure 20. DC anode current per tube throughout the acceleration cycle.

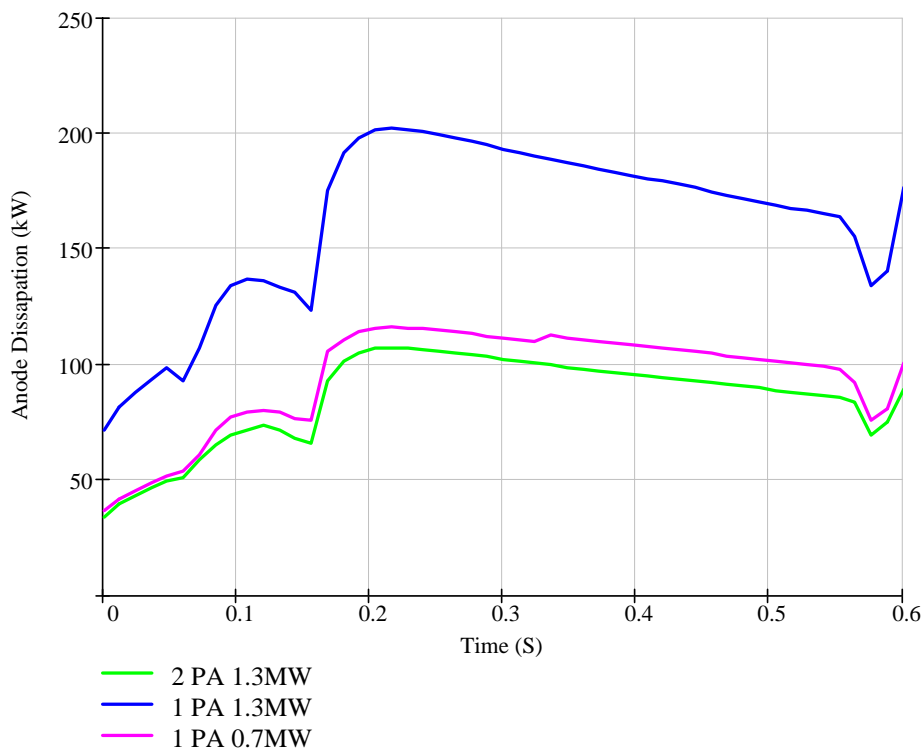


Figure 21. Anode dissipation thought the acceleration cycle.

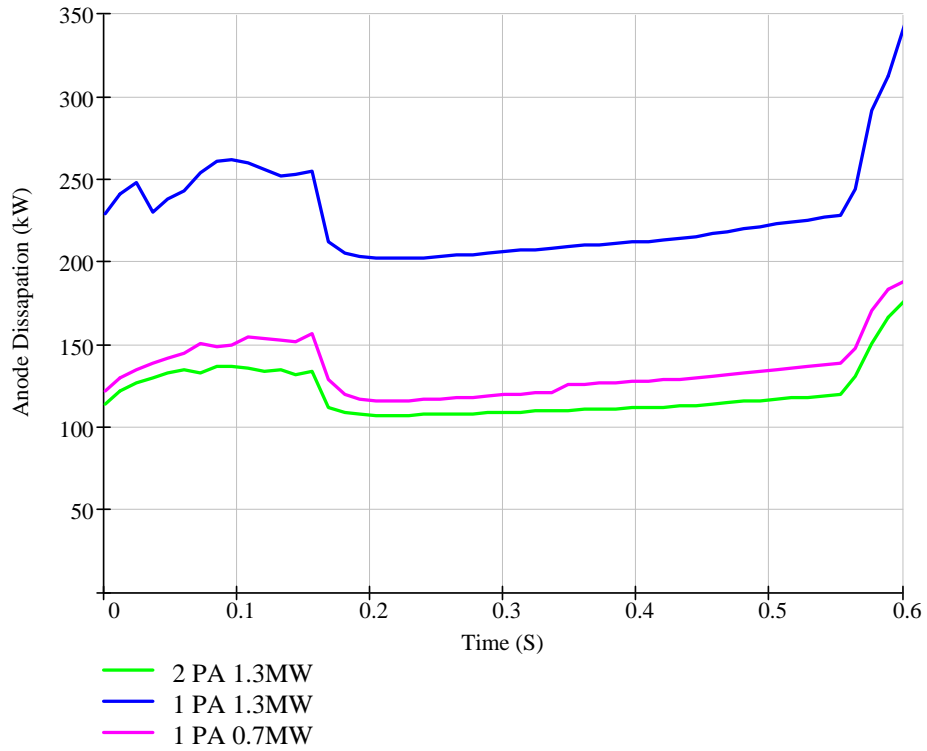


Figure 22. Anode dissipation for a constant anode voltage bias.

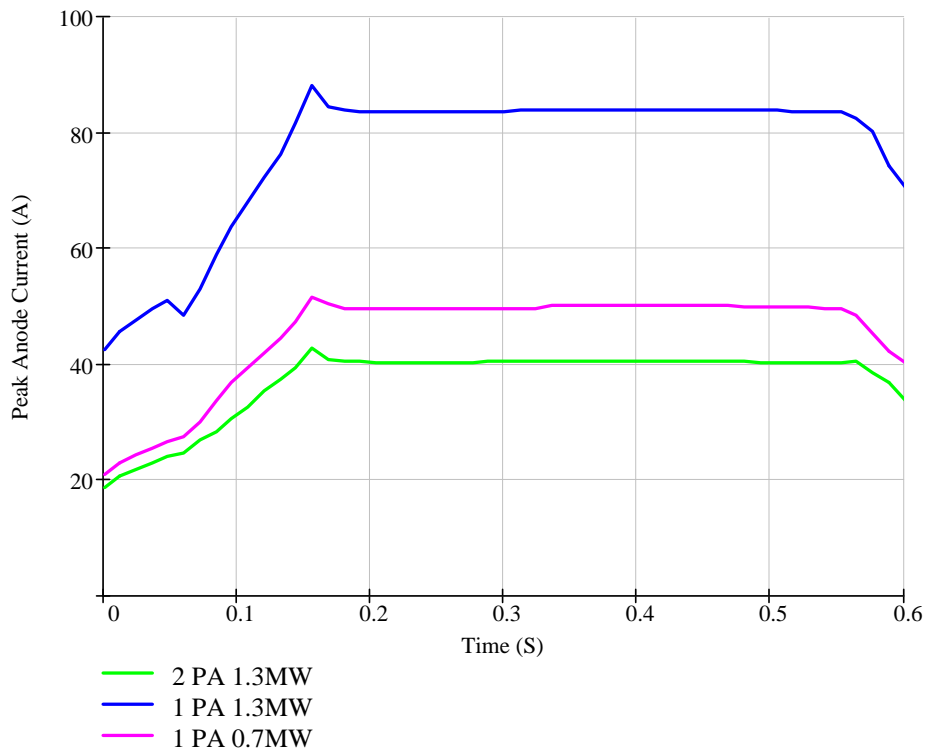


Figure 23. Peak anode current throughout the acceleration cycle.

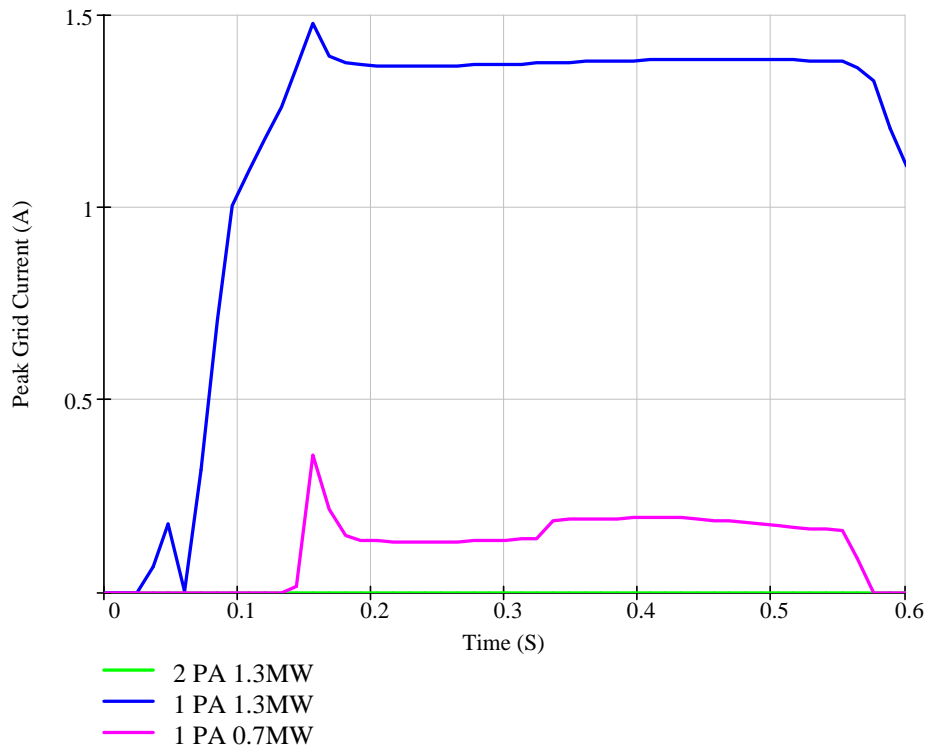


Figure 24. Peak grid current throughout the acceleration cycle.

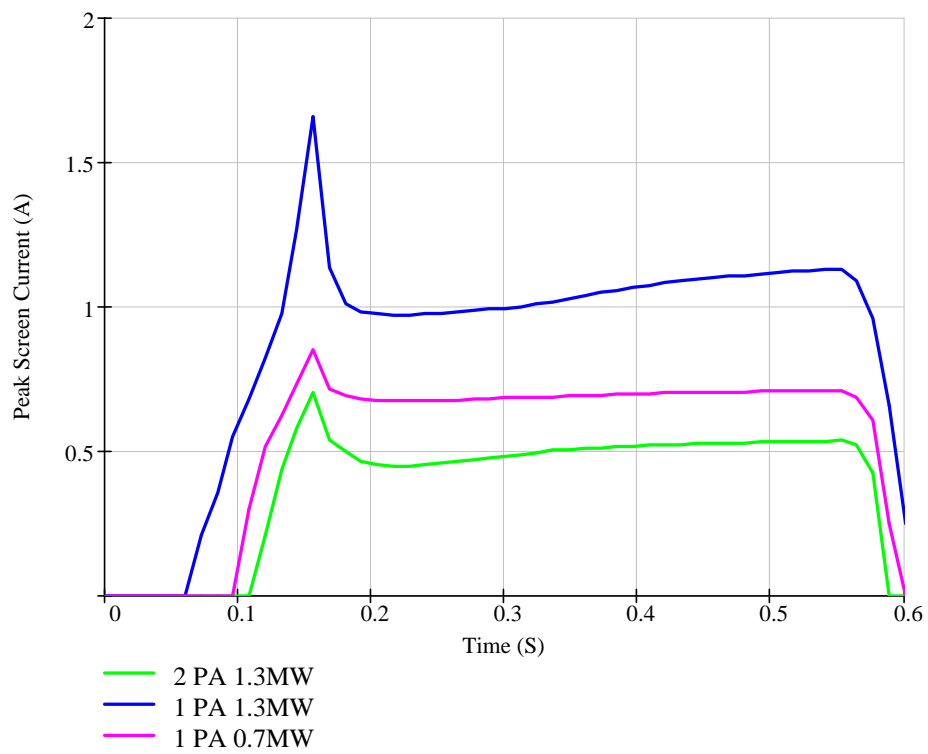


Figure 25. Peak screen current throughout the acceleration cycle.